한국해양환경공학회지
Journal of the Korean Society
for Marine Environmental Engineering
Vol. 11, No. 1. pp. 35-41, February 2008

월파형 파력발전장치 OWEC의 월류성능 수치해석

류 진[1,2] · 현범수[1,†] · 김길원[1]
[1]한국해양대학교 조선해양시스템공학부
[2]중국해양대학교 공과대학

Numerical Prediction for Overtopping Performance of OWEC

Zhen Liu[1,2], Beom-Soo Hyun[1,†] and Ji-Yuan Jin[1]
[1]Division of Naval Architecture & Ocean Systems Engineering, Korea Maritime University, Busan, Korea
[2]College of Engineering, Ocean University of China, Qingdao, China

요 약

월파형 파력발전장치는 월류된 파랑으로 인하여 발생한 수두차를 이용하여 터빈을 구동하는 일종의 파랑에너지 변환장치로써 파랑에너지를 전기 에너지로 변환하는 장치이다. 본 연구에서는 먼저 상용 CFD코드 인 Fluent를 사용하여 수치조파수조를 구현하고, Reynolds-Averaged Navier-Stokes 방정식과 VOF 모델을 이용하여 2차원 수치 선형 규칙파를 생성한 후 이를 계산 결과와 비교 검증을 수행하였다. 다음으로 월류 성능의 최적 설계점과 파력발전장치의 월류 충전량을 고찰하기 위하여 여러 가지 파랑조건과 형상변수들에 대하여 계산을 수행 하였다.

Abstract – Overtopping wave energy convertor is an offshore wave energy convertor for collecting the overtopping waves converting the water pressure head into electric power through the hydro turbines. This paper presents a numerical wave tank based on the commercial CFD code Fluent. The Reynolds Averaged Naiver-Stokes and VOF model is utilized to generate the 2D numerical linear propagating waves, which has been validated by the analytical solutions. Several incident wave conditions and shape parameters are calculated in the optimal designing investigation of the overtopping characteristics and discharge for the overtopping wave energy convertor.

Keywords: Wave energy(파랑에너지), OWEC(월파형 파력발전장치), Numerical wave tank(수치조파수조), VOF model(VOF 모델), Shape parameter(형상변수)

1. INTRODUCTION

The generation of electric power utilizing clean and renewable ocean resources is one of the most important alternative energy technologies for overcoming shortages in energy resources caused by excessive use of fossil fuels. Among various ocean resources, wave energy is most abundantly available and applicable in most coastal and offshore areas. Due to the advantages of simple converting technique and producing cost over other types of ocean energy, the wave energy conversion system is feasible to be established for the commercial power production.

Plenty of wave energy absorption devices have been invented, and several of them have been utilized in the electricity generation. Recently, the Oscillating Water Column (OWC) type has been widely employed in the application for the wave energy conversion. The disadvantage of this device is the low wave energy converting efficiency.

Overtopping Wave Energy Convertor (OWEC) has the sloping walls and reservoirs to lift waves to the levels above the average surrounding ocean. The released reservoir water is used to drive hydro turbines or other converting devices. OWEC has several distinct advantages over other types of wave energy converting devices. It produces

†Corresponding author: bshyun@hhu.ac.kr

a relatively small fluctuation in the derived electricity because it converts wave energy to potential energy in the calm water of the reservoir. Furthermore, OWEC is more feasible economically since it can be combined with other coastal facilities such as break waters.

TAPCHAN is the name of a prototype onshore generator that was installed on a remote Norwegian island in 1985 (L. Falnes *et al.* [1991]) and has been functioning ever since. The name is an abbreviation of "tapered channel", which describes the basic idea behind the device. TAPCHAN consists of a reservoir built into a cliff a few meters above the sea level. A tapered channel, which is wide at the mouth and open to the sea, becomes narrower as it penetrates the reservoir. Incoming waves increase in height as they move up the channel, eventually overflowing the lip of the channel and pouring into the reservoir. Wave Dragon (J. P. Kofoed *et al.* [2006]) is a floating wave energy converter of the overtopping type. It consists of two patented wave reflectors focusing the waves towards the ramp, linked to the wave reservoir. The wave reflectors have the verified effects of increasing the significant wave height substantially and thereby increasing the energy capture. Waves focused by the reflectors overtop the ramp and fill the reservoir, which is situated at a higher level than the surrounding sea.

The numerical simulation has become a very helpful tool in the investigation of the wave propagation and overtopping, especially in recent years. Reference (K. Hu *et al.* [2000]) presents a one-dimensional high-resolution finite volume model based on solving the non-linear shallow water equations capable of simulating storm waves propagating in the coastal surf zone and overtopping a sea wall. With the development of computer technology and computational dynamics methods, it is feasible to directly solve the Naiver-Stokes equations coupled with VOF model for the simulation of many problems, including the wave breaking and overtopping processes. The wave breaking and overtopping porous structures by using the Donor-acceptor VOF scheme are simulated in (M. Isob [2001]). As mentioned in (P. Lin and P.L-F. Liu [1998]), breaking waves in a surf zone by using a VOF based model are calculated to compare with the experimental data. A numerical two-phase flow model for incompressible viscous fluid proposed in (P. D. Hieu *et al.* [2004]) are utilized in the simulation of wave propagation in the shallow water, including the processes of wave shoaling, breaking, reflection and air movement.

In the present paper, a 2D numerical wave tank utilizing two-phase VOF model is established to study the overtopping characteristics and discharge for OWEC devices. It has been proved that VOF model can track the free surface and predict the air water interaction such as the air bubbles in the water and air dynamics on the free surface, which are important in the overtopping phenomenon. The Reynolds Averaged Naiver-Stokes (RANS) equations are employed as the governing equations. The standard turbulence model is applied to demonstrate the turbulent effects. The Finite Volume Method (FVM), Non-Iterative Time Advancement (NITA) - Pressure Implicit with Splitting of Operators (PISO) algorithm and dynamic mesh technique are used to generate the 2D linear propagating waves. Several incident wave conditions and shape parameters are calculated in the optimal designing investigation of the overtopping characteristics and discharge for the overtopping wave energy convertor.

2. MATHEMATICAL MODEL

2.1 Governing Equations

The schematic of a 2-D numerical wave tank is shown in Fig. 1. The propagating waves are generated by the wave maker plate at the left end, and the opening boundary is set at the other end.

The governing equations are the continuity equation and RANS equations for impressible fluid:

$$\frac{\partial u_i}{\partial x_i} = 0 \tag{1}$$

$$\frac{\partial u_i}{\partial t} + u_i\frac{\partial u_i}{\partial x_i} + u_j\frac{\partial u_i}{\partial x_j} = -\frac{1}{\rho}\frac{\partial p}{\partial x_i} + f_{x_i} + \frac{\partial}{\partial x_j}\left[\nu\frac{\partial u_i}{\partial x_j} - \overline{u_i'u_j'}\right] \tag{2}$$

where x_i, u_i represent the coordinate directions and corresponding velocity components; ρ, p, ν, f_{x_i} are the fluid density, the fluid pressure, the kinematic viscosity coefficient and the body force respectively.

The component $\overline{u_i'u_j'}$ defined as the Reynolds Stress induces a new turbulence model to close the equations. The

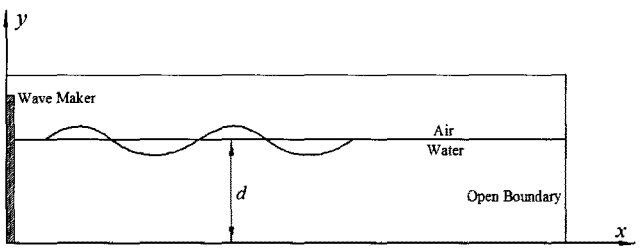

Fig. 1. Schematic of 2D Numerical wave tank.

standard k-ε model, which is widely used in engineering application, is employed in this study to demonstrate the turbulence effect in the wave motion.

The tracking of the interface between the air and water phases is accomplished by the Volume of Fluid (VOF) method. The volume fractions of water and air in the computational cell sum to unity. If the volume fraction of water is defined as a_w, then the following three conditions are possible: 1). a_w=0, the cell is empty of water; 2). a_w=1, the cell is full of water. 3). $0<a_w<1$, the cell contains the interface. The volume fraction a_w is computed as:

$$\frac{\partial a_w}{\partial t}+\frac{\partial (a_w u_i)}{\partial x_i}=0 \tag{3}$$

In addition, the face fluxes through the computational cells are obtained as the geometric reconstruction approach. The interface between two fluids is calculated by the piecewise-linear scheme, which assumes the linear slope in each cell.

2.2 Numerical Solutions

The regular linear wave is employed in the investigation of this paper, and the motion of the piston wave maker is determined from the following equation:

$$x(t)=\frac{S_0}{2}\left(1-e^{-\frac{5t}{2T}}\right)\sin\omega t \tag{4}$$

where S_0 is the maximum displacement of the wave maker; T is the period of incident wave, and $\omega = 2\pi/T$.

On the opening boundary, the Sommerfeld radiation boundary condition, which has good capability of linear wave absorption, can be written as:

$$\frac{\partial \phi}{\partial t}+c\frac{\partial \phi}{\partial x}=0 \tag{5}$$

where ϕ is velocity potential and c is wave velocity. Substituting Eq. (5) for the dynamic boundary condition of the free surface in the linear wave theory, the relation between the horizontal velocity component and the free surface elevation is obtained:

$$u=\frac{g\eta}{c} \tag{6}$$

where $u=\partial\phi/\partial x$ denotes the horizontal velocity, η the free surface elevation and g the gravity acceleration. The wave absorption can be performed by controlling the motion of the opening boundary.

The motion of the wave generating and absorbing boundaries can be achieved by defining UDF (User-Defined Function) programs. Fluent also provides the layering remeshing method in dynamic mesh model to govern the mesh reconstruction adjacent to the moving boundaries. The geometry and meshes are created by Gambit, and it should be noted that the grids at the interface has been refined to predict the free water surface precisely.

The governing equations are solved by using Finite Volume Method. Second-order upwind discretization is considered for the convection terms. The pressure-velocity coupling is calculated by the NITA (None-Iterative time advancement) - PISO (Pressure Implicit with Splitting of Operators) algorithm compatible with VOF model, which requires only one global iteration per time step, and reduces solution time significantly.

In Fluent, Symmetry definition is applied for the wave making and absorbing boundaries. The bottom is set as the wall using no-slip conditions. The pressure outlet is considered for the upper boundaries of the computational domain adjacent to the air phase.

2.3 Validation of VOF Model

The two-dimensional dam break problem is a very useful benchmark test. The test provides extreme conditions to assess the numerical stability, as well as the capability of the model to treat the free surface problem.

The problem of a dam break over a dry bed is investigated, and the computed results are compared with the laboratory experimental data of (J. C. Martin and W. J. Moyce [1952]). In the experiment as given in Fig. 2, a rectangular column of water in hydrostatic equilibrium is confined between two vertical walls. The water column is two-unit high and

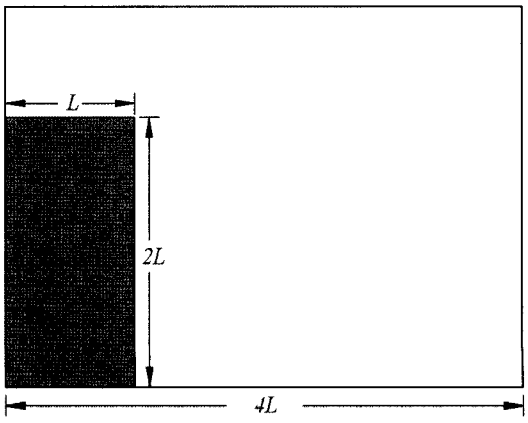

Fig. 2. Schematic of the dam break over a dry bed.

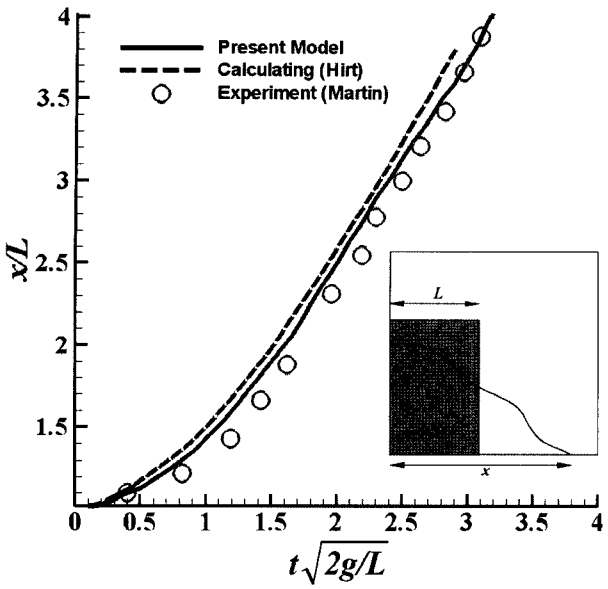

Fig. 3. Time history of the position of the leading edge of waver.

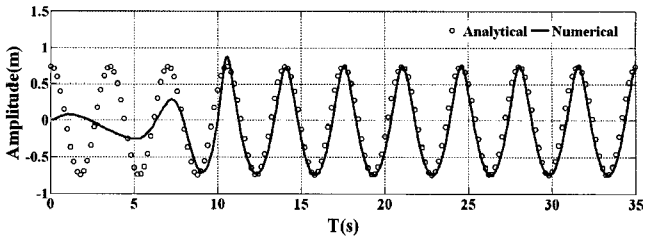

Fig. 4. Time series of wave elevation at the position of $x = 25$ m.

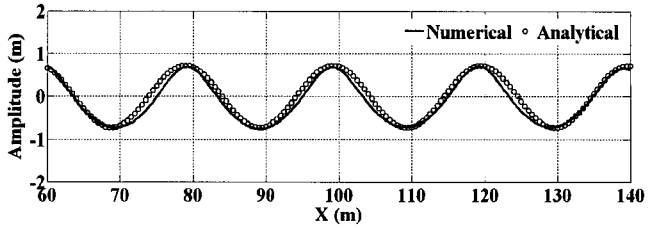

Fig. 5. Comparition of wave profile at $t = 23\ T$.

one-unit wide. The gravity force is acting downward. At the beginning of the experiment, the dam is instantly and totally removed and the water is allowed to flow out along the horizontal floor.

In the numerical simulation, a square computation domain with the length and height equal to 22.8 cm is set. A water column with the width L and height 2L (L=5.7 cm) is assumed at the left side of the computation domain. The comparison between computed dimensionless positions of the leading edge of the water and the experimental data (J. C. Martin and W. J. Moyce [1952]) is shown in Fig. 3. As shown in the figure, the calculated results agree well with the experimental data, and thus the model shows its ability for the simulation of free surface problem. It also can be seen in the figure that the calculated results by the present model are more accurate than those by the SOLA-VOF code (C. W. Hirt and B. D. Nichols [1981]).

2.4 Validation of Numerical Wave Tank

A rectangular wave tank with flat bottom is set up to validate the capability of the numerical model described in this paper. The tank length is 200 m, and the water depth is 16 m. The maximum displacement of wave maker is S_0=0.8 m, and the incident wave period is T=3.5 s. The calculating time step is taken as 0.001s.

The numerical results for the time series of wave elevation at the position of $x = 25$ m and their comparisons with the corresponding analytical solutions are shown in Fig. 4. It can be seen that the numerical results of present model agrees well with the linear solutions after the initial transient effect has diminished.

Fig. 5 illustrates the computation for the distribution of wave profile along the tank at $t = 23\ T$. The results obtained by the present method show fairly good agreement with the linear wave solutions. It also can be found that the wave elevations in the numerical prediction are slightly smaller in magnitude than the analytical solutions as the wave propagates in the tank. The results obtained by the present method show fairly good agreement with the linear wave solutions. It also can be found that the wave $t = 23\ T$.

All the above results indicate that the 2-D numerical wave tank developed in this paper can generate the propagating regular waves within desired wave heights and periods for the engineering applications.

3. INVESTIGATION OF OWEC

The 2D schematic of a typical OWEC device are given in Fig. 6. It consists of a reservoir to store water and the

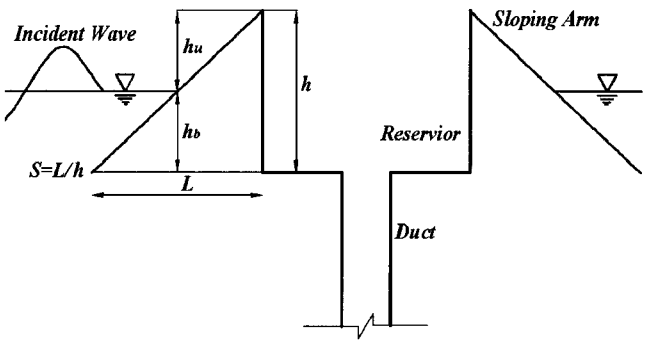

Fig. 6. 2D Schematic of OWEC.

Table 1. Testing cases with variation of sloping ratio and incident wave conditions

Case	S	H(m)	T(m)	Case	S	H(m)	T(m)
01	1:1	1.0	4.0	07	1:1	2.0	4.0
02	1:1	1.0	6.0	08	1:1	2.0	6.0
03	2:3	1.0	4.0	09	2:3	2.0	4.0
04	2:3	1.0	6.0	10	2:3	2.0	6.0
05	1:2	1.0	4.0	11	1:2	2.0	4.0
06	1:2	1.0	6.0	12	1:2	2.0	6.0

sloping arms for the waves to run up from the incident directions. The device is fixed to the sea bottom by the duct installed with the low head hydro turbines.

As shown in Fig. 6, L and h represent the length and height of the sloping arm, respectively. The sloping ratio S of the device arm is defined as: $S=L/h$. h_u is the hydro head, and h_b is the underwater height of the sloping arm. In the present study, the water depth is 20 m. h_u and h_b are both fixed as 2 m. Therefore, the length of the device arm varies with respect to the variation of the sloping ratio S.

In the present study, the wave heights H=1.0 m, 2.0 m and wave periods T=4.0s, 6.0s are utilized as the incident wave conditions. The sloping ratios of the device arm are set as 1:1, 2:3 and 1:2. The testing cases are summarized in Table 1.

4. RESULTS AND DISCUSSION

In the numerical investigation, the OWEC device without the duct is employed because the investigating emphasis is the overtopping characteristics and discharge amount.

The length of the numerical wave tank is 300 m, the OWEC device is 200 m from the wave maker at the left end. The opening boundary is set at the right end of the flume.

The process of wave running up over the OWEC in one incident wave period for Case 01 is shown in Fig. 7. The sloping ratio is 1:1 and the incident wave height is 1.0 m. It can be seen from the figure that the waves will not break during running up the sloping arm of the device, and they cannot overtop and fall into the reservoir. The overtopping phenomenon also cannot be found in Case 2~6. It comes from the difference between the high hydro head hu and the low incident wave height. The above numerical results indicate that the difference between the hydro heads and incident wave heights is quite important for the overtopping of OWEC.

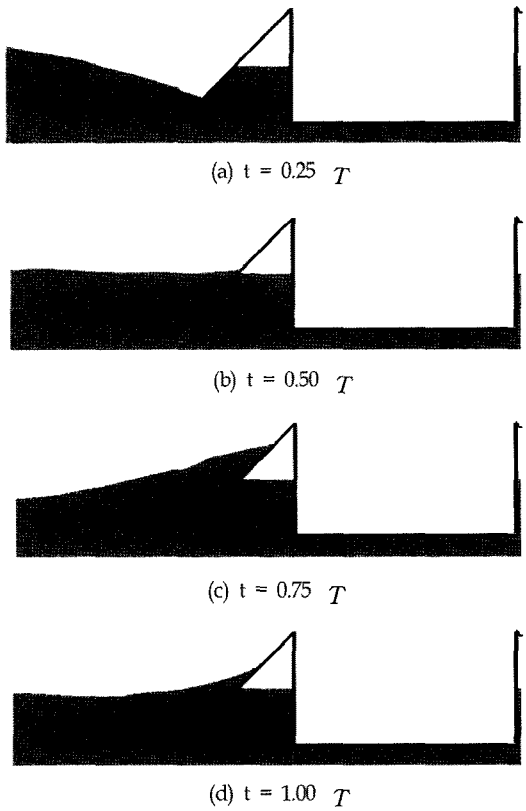

Fig. 7. Snapshot of wave run up in one period Case 01.

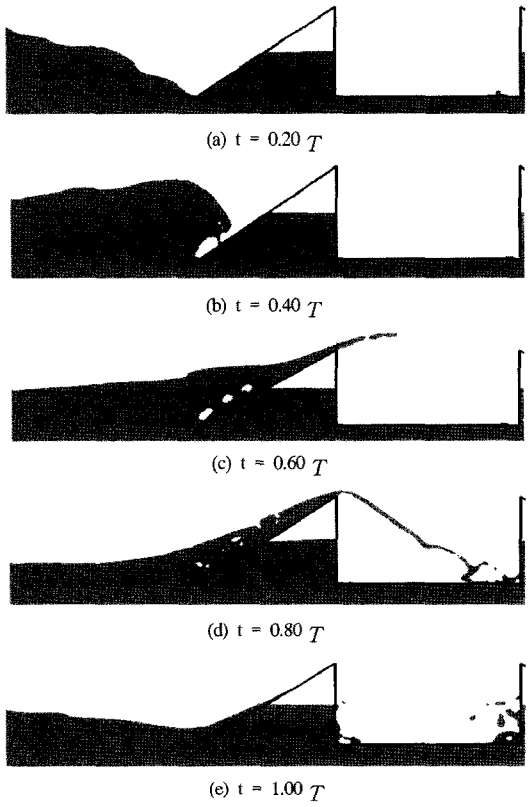

Fig. 8. Snapshot of overtopping in one period for Case 10.

The process of wave overtopping the OWEC device in one incident wave period for Case 10 is given in Fig. 8.

The sloping ratio S is 2:3, and the incident wave height H is 2 m. As shown in Fig. 8(a) and (b), the incident waves are blocked by the sloping arm and break during climbing up the arms. The air bubbles are also enclosed in the water in Fig. 8(c). The overtopping water will splash in the reservoir and cause the energy loss. The overtopping phenomena in the other cases also show the similar behavior ignoring the incident wave periods.

The above results demonstrate that the ratio of the incident wave heights to the hydro head of the devices is critical to the overtopping capability of OWEC. The small sloping ratios also cause the overtopping water splash in the reservoir and energy loss.

The time series of the flow rate of waves overtopping into the reservoir for Case 12 are shown in Fig. 9, which can be monitored by Fluent at the proper position. The overtopping flux is obviously smaller because of the less wave height of the first arriving wave. The maximum values of the overtopping fluxes of the later arriving waves are similar, which evidently larger than the first wave. It also can be seen that the variation period of the overtopping fluxes are same as the incident wave period. The overtopping flow rates of the other cases also show the similar variation behaviors.

The overtopping discharge can be obtained by integrating the flow rate curve in Fig. 9, which is displayed in Fig. 10. The variations of overtopping discharges are stable after the initial effects of the first arriving wave.

The operating performance of OWEC device is determined by the overtopping discharge of the water column because it represents the potential energy contained by the

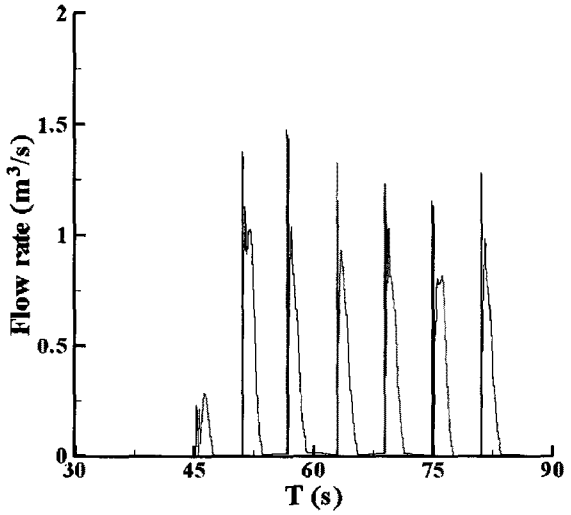

Fig. 9. Time series of overtopping flow rate of Case 12.

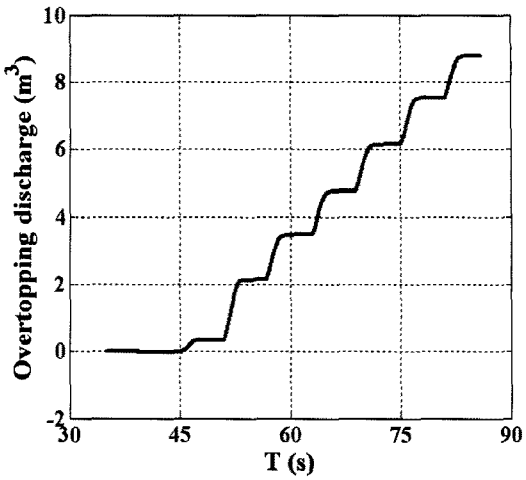

Fig. 10. Time series of overtopping discharge of Case 12.

Table 2. Comparison of overtopping discharges for Case 07~12

Case	Overtopping discharge in one period (m^3)	Overtopping discharge in 12 s (m^3)
07	0.587	1.761
08	1.194	2.389
09	0.653	1.960
10	1.336	2.673
11	0.959	2.877
12	1.465	2.929

water column in the reservoir, which can be converted to the kinetic energy of the falling water to drive the hydro turbines.

The overtopping discharges for Case 07~12 are shown in Table 2. It can be seen that the overtopping discharges in one period within the incident wave period T=4.0s is smaller than that of the period T=6.0s for every sloping ratios. On the other hand, the overtopping discharges within the same incident will increase as the sloping ratios reduce. The numerical prediction shows that the smaller sloping ratios S will increase the overtopping performance of the OWEC devices.

In order to compare the overtopping performance of OWEC within various periods relatively, the operating period is chosen as 12s. In this operating period, there are 3 waves for T=4.0s and 2 waves for T=6.0s. The calculating results show that the overtopping discharges for T=6.0s in an operating period are larger than those for T=4.0s when the sloping ratio is large. The difference of the overtopping discharges between T=6.0s and T=4.0s is minor.

5. CONCLUSIONS

A 2D numerical wave tank utilizing two-phase VOF model is established to study the overtopping characteristics

and discharges for the Overtopping Wave Energy Convertor. The propagating regular waves generated by the numerical wave tank show the agreement with the linear analytical solutions. The VOF model is also validated by the experimental data for the dam break problem.

Several shape parameters and incident wave conditions are tested using the present numerical wave tank. It can be seen that there are no overtopping phenomena with the incident wave height H=1.0m. For the wave height H=2.0m, the sloping ratios have evident effects on the operating performance of OWEC. The overtopping discharges for every sloping ratio will increase as the incident wave period increases in a incident wave period. The overtopping discharges within small incident wave periods in one operating period are smaller than those within larger wave periods. When the sloping ratio decreases, the effect of the incident wave periods is minor.

ACKNOWLEDGMENT

This research is supported by the Korea Energy Management Corporation through Korea Ocean Research & Development Institute (KORDI). All the supports are gratefully acknowledged.

REFERENCES

[1] Falnes, L. and Loveseth, J., 1991, "Ocean Wave Energy", Energy Policy, Vol. 19, No. 8, pp. 768-775.

[2] Hirt, C. W. and Nichols, B. D., 1981, "Volume of fluid (VOF) method for the dynamics of free boundaries", J. Comput. Phys., Vol. 39, pp. 201-225.

[3] Hu, K., Mingham, C. G. and Causon, D. M., 2000, "Numerical simulation of wave overtopping of coastal structures using the nonlinear shallow water euqations", Coastal Engineering, Vol. 41, pp. 433-465.

[4] Hieu, P. D., Katsutoshi, T. and Ca, V. T., 2004, "Numerical Simulation of breaking waves using a two-phase flow model", Applied Mathematical Modeling, Vol. 28, pp. 983-1005.

[5] Isobe, M., 2001, "A VOF-based numerical model for wave transformation in shallow water", In proc. Int. Workshop on ADMS21, PHRI, pp. 200-204.

[6] Kofoed, J. P., Frigaard, P., Madsen, E. F., and Sorensen, H. C., 2006, "Prototype testing of the wave energy converter wave dragon", Renewable Energy, Vol. 31, pp. 181-189.

[7] Lin, P. and Liu, P. L-F., 1998, "A numerical study of breaking waves in the surf zone", J. Fluid Mech. Vol. 359, pp. 239-264.

[8] Martin, J. C. and Moyce, W. J., 1952, "An experimental study of the collapse of liquid columns on a rigid horizontal plane", Philos. Trans. Roy. Soc. London, Ser. A, Vol. 244, pp. 314-324.

2007년 10월 15일 원고접수
2008년 2월 11일 수정본 채택